Molecular design and QSAR study of low acute toxicity biocides with 4,4′-dimorpholyl-methane core obtained by microwave-assisted synthesis†

Raúl Hernández-Altamirano,[a] Violeta Y. Mena-Cervantes,[a] Sandra Perez-Miranda,[d] Francisco J. Fernández,[d] Cesar Andres Flores-Sandoval,[b] Victor Barba,[e] Hiram I. Beltrán*[f] and Luis S. Zamudio-Rivera*[c]

The solventless microwave-assisted synthesis of aldehydes (**1a**, **2b–h**) and morpholine (**3**) in 1 : 2 (aldehyde : morpholine) ratio yielded eight 4,4′-dimorpholyl-methanes (**4a–4h**), which were thoroughly characterized through FT-IR, ^{1}H, ^{13}C and 2D NMR, confirming structures of type **4**. The described compounds are dimorpholino-methane (**4a**), 2-(dimorpholinomethyl)-phenol (**4b**), 4-bromo-2-(dimorpholinomethyl)-phenol (**4c**), 2,4-di-*tert*-butyl-6-(dimorpholinomethyl)-phenol (**4d**), 4,4′-(pyridin-2-ylmethylene)-dimorpholine (**4e**), 4,4′-((4-*iso*-propylphenyl)methylene)-dimorpholine (**4f**), 4,4′-(naphthalen-1-ylmethylene)-dimorpholine (**4g**) and 4,4′-(pyren-1-ylmethylene)-dimorpholine (**4h**). Additionally, single crystal X-ray diffraction analysis for **4b**, **4c**, **4d** and **4e** derivatives was accomplished showing interesting geometrical features. The obtained 4,4′-dimorpholyl-methanes were subjected for two biological tests, (i) acute toxicity, related to *Photobacterium phosphoreum* (*Vibrio fischeri*), and (ii) biocidal activities, determined for *B. subtilis*, *E. coli* and *Ps. fluorescence* strains. The results show that **4a–h** compounds have varying degrees of toxicity, classified as **4a**, **4b**, **4c**, **4e** and **4f** as slightly to moderately toxic agents, **4g** and **4h** as highly toxic chemicals, and **4d** as an extremely toxic compound. Besides, the biocidal activities, which is controlled mainly by the substituent directly bonded to the methinic bridge (named C5, which originally is the carbon atom of the aldehyde functionality), have shown varying degrees of inhibitory effects on the growth of selected strains, depending on the chemical structure of **4a–h**. A QSAR study was developed, and quantum-chemical parameters of **4a–h** were obtained with the DFT approach at the B3LYP/6-311G(d) level of theory in the gas phase. Hence ten molecular descriptors were determined, being E_{HOMO}, E_{LUMO}, GAP, C5 Mulliken atomic charge (AC$_{Mulliken}$), C5 atomic charge of NBO (AC$_{NBO}$), dipolar moment (μ), molecular hydrophobicity as log P, molecular volume (Vol), electrostatic potential (ESP) and δ^{13}C(C5), all of them being typical determinants of biological activities in other, different or related, molecular systems. A linear combination from three to six molecular descriptors was chosen as a multivariate model to achieve correlations in order to relate them to their acute toxicity and understand the obtained trend. Three sets of descriptors accomplished the statistical goal, and through an identity analysis the conserved descriptors in these three series are log P, the ESP and the δ^{13}C(C5), which seemed to be the tracking variables in the system. To a lesser extent, the frontier orbitals and their relations (HOMO, LUMO and GAP) are also present within the correlations. The phenol-bearing structures (**4b**, **4c** and **4d**, derived from salicylidenes) are best tuned within these variables since the substitution in the phenol fragment both governs the toxicity and the biocidal potency. Finally, we can guarantee that the best candidates in this series are **4a**, **4b** and **4c**, because diminished toxicity and preserved biocidal potency were obtained at the same time. A more hydrophobic substitution (**4d**) extremely increases the *Vibrio fischeri* toxicity, ruling out its application. Through the full analysis presented in this piece of work it can be stated that selected prototypes could be used in industrial facilities, particularly in the petroleum industry, as a new generation of ecological chemical products.

[a]Posgrado, Instituto Mexicano del Petróleo, Eje Central Lázaro Cárdenas No. 152, Apartado Postal 14-805, 07730, México, D.F.
[b]Programa de Ingeniería Molecular, Instituto Mexicano del Petróleo, Eje Central Lázaro Cárdenas No. 152, Apartado Postal 14-805, 07730, México, D.F.

[c]Laboratorio de Síntesis Química y Electroquímica, Instituto Mexicano del Petróleo, Eje Central Lázaro Cárdenas No. 152, Apartado Postal 14-805, 07730, México, D.F.. E-mail: lzamudio@imp.mx
[d]Departamento de Biotecnología, DCBS, Universidad Autónoma Metropolitana-Iztapalapa, Apartado Postal 55-535, 09340, México, D.F.

Introduction

It is well known that certain kinds of anaerobic as well as aerobic bacteria commonly present in operation fields of petroleum industry can generate or have influence on corrosion processes over the plant installation systems. In this sense, it is worthwhile mentioning the employed terminology stating that "*Microbiological corrosion is the deterioration of materials caused directly or indirectly by bacteria, algae, moulds or fungi; singly or in combination.*"[1] In order to keep microbiological corrosion under control, chemical substances, ordinarily known as biocides, have been used in oil field operation systems. These biocides are active substances able to eliminate or at least inhibit such microorganisms at their reproductive cycle, growth or by both mechanisms.[2,3]

Among the main types of biocides applied in the oil industry are quaternary ammonium and phosphonium salts (*e.g.* of ionic liquid behaviour), isothiazoline and heavy metal salts, *etc.* Although these compounds have good efficiency they also have the inconvenience of being non-selective, highly toxic and as a result they cannot fulfil the ecologic requirements recently established by international legislation.[4] In order to find out more green chemicals of this type, some researchers have proposed and tested the potential of ionic liquid-based compounds resulting in low toxicity in aquatic[5–7] as well as in cell-based tests,[8] which was highly dependent on small molecular structure variations. Additionally, quite similar ionic liquids to those tested for toxicity have been studied for oilfield applications regarding the findings of desirable physicochemical properties into these industrial tasks.[9,10] Hence, this type of chemical prototype should be applied as potential biocides in the control of harmful aquatic organisms, as has been recently reported.[11–13] These efforts direct the search for new structural motifs as well as to give a further view for gathering emerging knowledge in the area of rationale design of molecules for biological applications[5,6,8,13–21] in aquatic and other media, such as oil, and towards different types of organisms.

The high toxicity of the majority of biocides precludes their use[22] and the development of new candidates with diminished toxicity but maintaining their performance is hence needed. Due to those important points defined in the introductory section, the aim of this work is to assess the antimicrobial activity, defined as biocide potency, as well as the *Vibrio fischeri* toxicity levels of 4,4′-dimorpholyl-methane compounds, against several *"model microorganisms"* and *"corrosion participating microorganisms"*, to provide insights about their application as biocides of low acute toxicity. These 4,4′-dimorpholyl-methane-based biocide prototypes, are easily synthesized and highly efficient, fulfilling the established toxicity criteria for this kind of substances. Indeed, due to their chemical structure, they also resemble prototypes for obtaining ionic liquids, such as those reported elsewhere, that have shown to posses controllable toxicity levels.[5–7,11–13,23] During the molecular design of these com-

pounds it was observed that small structural changes directly affected the desired properties.[11] In order to ascertain chemical structures and correlate this with their biological evaluations we describe the structural and spectroscopic characterization of a series of 4,4′-dimorpholyl-methanes. Their activities have been measured against aerobic bacteria (*Bacillus subtilis*, Gram-positive, strain ATCC 6633; *Escherichia coli*, Gram-negative, strain DH5R; and *Pseudomonas aeruginosa*, Gram-negative, strain BH3). The acute toxicological activity of each compound was measured using the Microtox luminescent bacteria toxicity (LBT-Microtox) test; the sensitive *Photobacterium phosphoreum* (*Vibrio fischeri*) was used as the standard,[24] instead of other mammalian cell lines,[8,25] because of the simplicity of the microorganisms, their acute responses, and their methodical and confident, and reliable, use compared to other more expensive and developed toxicity tests. The comparative study allowed us to identify a thorough relationship between activity and structure for these simple but promising molecules.[7]

Quantitative structure–activity relationship (QSAR) and quantitative structure–property relationship (QSPR) models correlate molecular structures with a measured activity or property using molecular descriptors of many sources, both of experimental and theoretical nature, attempting to capture the relationship between the chemical and physical information in the descriptors with that of activity (biological, industrial, pharmaceutical, *etc.*).[26,27] The thorough management of the latter allows a property to be predicted or approached independently of having a complete knowledge of its origin. The QSAR has been developed to assess the *Vibrio fischeri* toxicity for different chemicals based on the reactivity and structure.[23,25] Nuclear magnetic resonance (NMR) spectroscopy is the most powerful method in analytical chemistry for the identification of structural groups, molecular structures and their inherent information. ^{13}C NMR spectra have been employed in several QSAR and QSPR studies,[28] where different methods have been used to include NMR descriptors. However one of the simplest NMR descriptors or indexes is the chemical shift of a common structural nucleus, often employed to track a particular behaviour. At the same time, for our own purposes, we calculated some other descriptors by means of density functional theory (DFT) or semiempirical (PM3) approaches, *e.g.* highest occupied (E_{HOMO}) and lowest unoccupied (E_{LUMO}) molecular orbitals and their difference (GAP) in absolute value, dipole moment (μ), partition coefficient (log P), Mulliken atomic charge (AC_{MK}), atomic charge derived from Natural Bond Orbital analysis (AC_{NBO}), electrostatic potential (ESP), *etc.* These indexes were statistically tested in order to find QSAR through least squares minimization. The chosen QSAR model was a linear combination of molecular descriptors due to its simplicity of construction and analysis. These selections gave good results in this case of study and gave insights in the rational design of chemicals for biological applications, as will be seen.

Results and discussion

Microwave assisted synthesis and spectroscopic characterization of 4,4′-dimorpholyl-methanes

The reaction between paraformaldehyde (**1a**) or selected aromatic aldehydes (**2b–h**), and morpholine (**3**) (Scheme 1) was

ᶜCentro de Investigaciones Químicas, Universidad Autónoma del Estado de Morelos, Av. Universidad 1001, 62210, Cuernavaca, México

ᴶDepartamento de Ciencias Naturales, DCNI, Universidad Autónoma Metropolitana-Cuajimalpa, Pedro Antonio de los Santos 84, Sn. Miguel Chapultepec, 11850, México, D.F.. E-mail: hbeltran@correo.cua.uam.mx
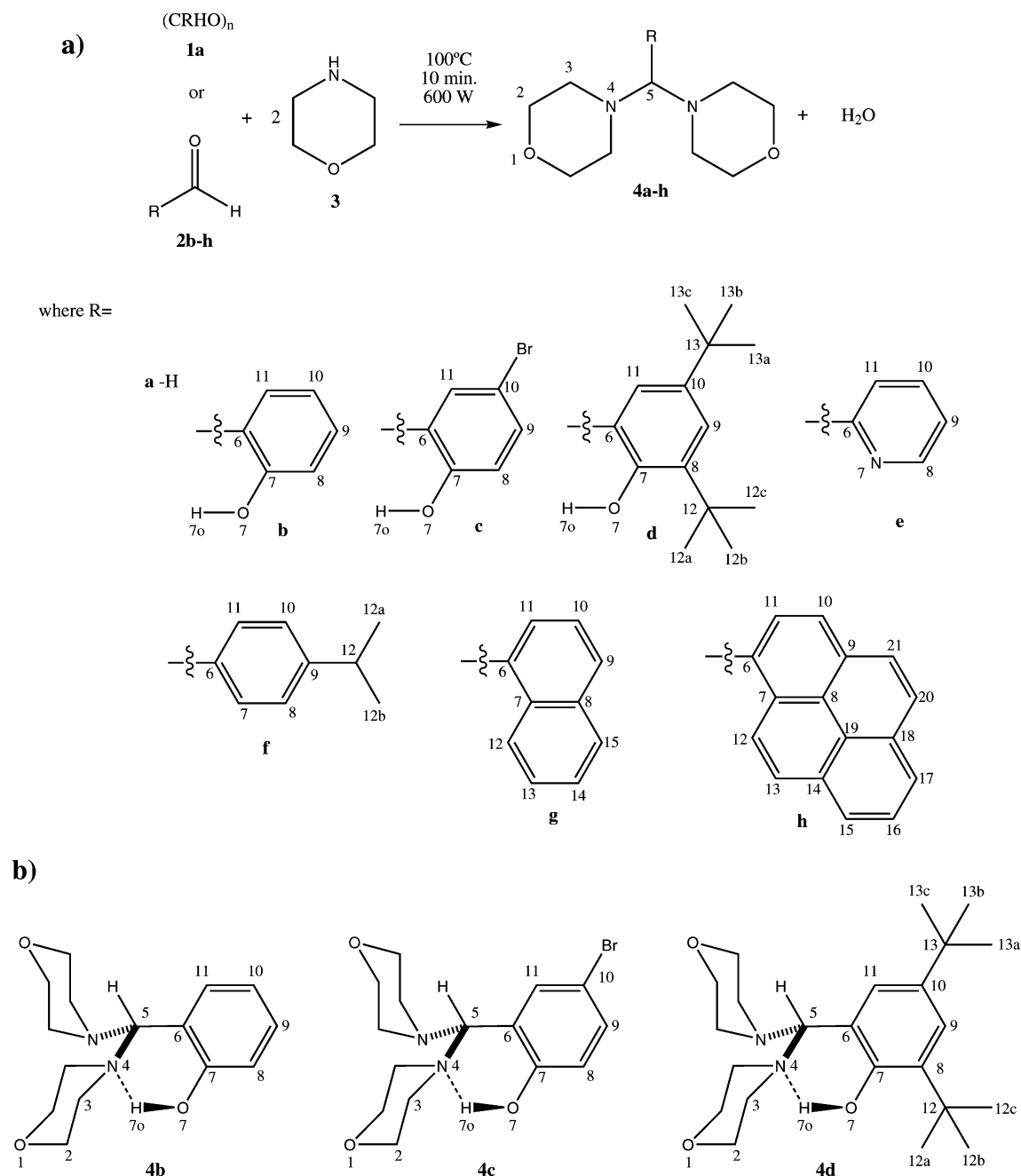
Scheme 1 (a) Solventless microwave assisted reaction of aldehydes (**1a**, **2b–h**) with morpholine (**3**) to obtain compounds **4a–h**. (b) Hydrogen bonding present in compounds **4b**, **4c** and **4d**.

carried on in a reactor using 600 W of microwave irradiation power,[29] setup temperature of 100 °C, over a period of 10 min. This reaction scheme was general and thus applied to all selected reagents, which led to eight different biocide prototypes (**4a–h**) in yields ranging from 65 to 98%. For ecological reasons, all reactions were carried out in the absence of any solvent, employing a microwave irradiation system. The reactions only produced water as an additional product, besides the desired **4a–h** compounds.

Spectroscopic characterization of 4a–h

The ^{1}H, ^{13}C as well as HETCOR and COSY standard pulse sequences (from Varian) were employed to obtain the desired spectra. The analysis of ^{1}H and ^{13}C spectra revealed the molecular symmetry present (C_{2v}) in solution with almost freely rotating morpholine rings (details of these findings are discussed below). The integration of the ^{1}H nuclei signals gave 2 : 1 intensities for the morpholine moiety compared with that belonging to the

original aldehyde fragments, also giving evidence of the integrity of the desired products. In all cases the ^{1}H NMR spectra revealed the same pattern for the morpholine moiety at position 2, and appeared between 3.67 and 3.72 ppm. Meanwhile the axial and equatorial proton nuclei at position 3 appeared averaged for **4a–d** and **4f** between 2.43 and 2.59 ppm. A particular behaviour was observed for **4e**, **4g** and **4h**, where the hydrogen nuclei present at position 3 have different chemical shifts, showing that the equatorial and axial positions are not averaged, providing chemical and magnetic differences. The axial hydrogen nuclei (H3) appear between 2.44 and 2.54 ppm, and the equatorial ones appear between 2.55 and 2.62 ppm. This observation suggests a fixed orientation for the nitrogen atom and a fluctuating positioning of the oxygen atom, both at the morpholine moiety, as depicted in Scheme 2. For the **4** series, H-5 appears at 2.91 ppm for **4a**, and in all other cases this is shifted to higher frequencies due to the presence of an *ipso* aromatic moiety. This effect moved the positions depending on the pendant group: 3.77 for **4b**, 3.72 for **4c**, 3.75 for **4d**, 3.88 for **4e**, 3.61 for **4f**, 4.60 for **4g** and 4.91 for **4h** (all in ppm). In the case of ^{13}C NMR shifts, a similar tendency was observed. A constant appearance of three carbon signals for the positions 2, 3 and 5 was evidenced in intervals of 66.7–67.2 (C2), 49.3–51.8 (C3) and at 81.5–90.4 (C5), all in ppm. The latter nuclei are more affected, due to the character of the pendant group, as stated also for the ^{1}H nuclei. The remaining ^{13}C signals, of aromatic type, are shifted depending on the particular substitutions of each group. Also the FT-IR spectra revealed the expected bands, and in all cases those corresponding to the starting materials were absent, such as those of the original aldehydes (**2b–h**) or the starting amine (**3**).
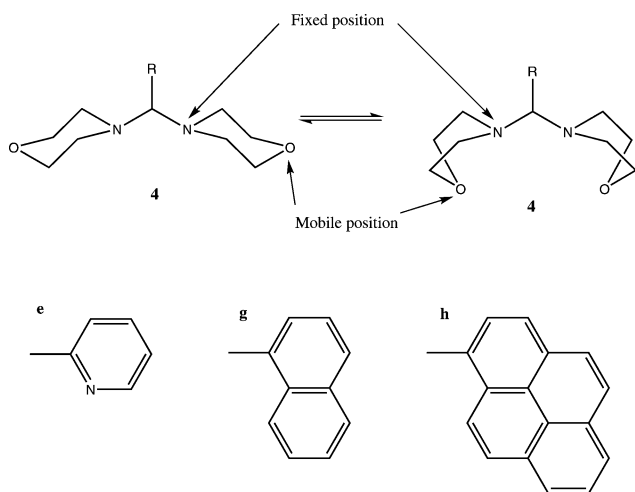
Scheme 2 Restricted fluctuating behaviour observed in the ^{1}H NMR spectra for **4e**, **4g** and **4h** in CDCl$_3$ solution at 25 °C.

X-Ray crystal structure determination

Compounds **4b**, **4c**, **4d** and **4e** were successfully crystallized and their structures were determined by single-crystal X-ray diffraction analysis, as shown in Fig. 1, and the structural numbering in this section is in accordance with that reported in this figure. Table 1 gathers the results of data collection and selected geometrical parameters are shown in Table 2 (including the hydrogen bonding scheme for **4b**, **4c** and **4d**). Compounds
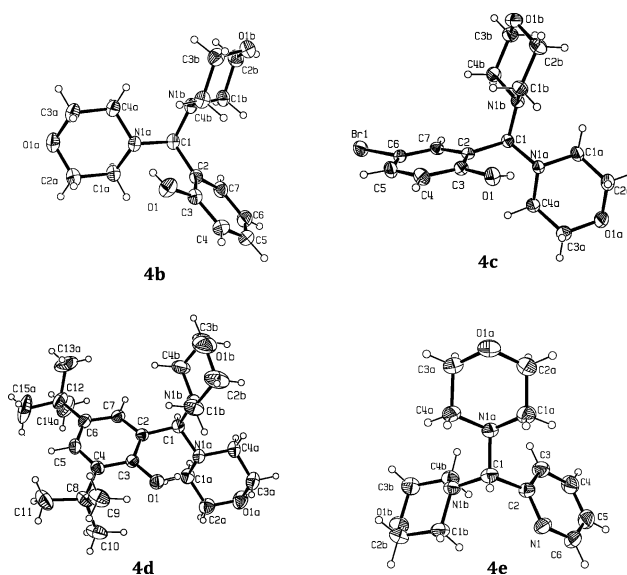

Fig. 1 X-Ray structures of **4b–4e** and the hydrogen bonding present in **4b–d**. Ellipsoids were drawn at 30% of probability. The most representative part of the disorder in **4d** (part A of the contribution) was used for drawing purposes.

4b and **4c** crystallized as orthorhombic systems while **4d** and **4e** are present as monoclinic systems. The neighbour N1A···N1B contact distances, due to double addition of morpholine to the carbon atom originally belonging to the aldehyde precursor, are 2.407(3) for **4b**, 2.393(3) for **4c**, 2.402(2) for **4d** and 2.394(2) for **4e** (all in Å), and fall within the same range with small variations due to structural changes. For compounds **4b**, **4c** and **4d**, a hydrogen bonding interaction is present, since they came from a salicylaldehyde fragment and its *ortho* hydroxyl group in responsible for such an interaction, thus providing a good Brønsted donor group. Once the current compounds are formed, the hydrogen bonding has been observed between H1o and N1A. The bond distances (in Å) between H1o (of O1) and N1A are 1.99(3) for **4b**, 1.99(3) for **4c** and 1.74(2) for **4d**, shorter that the sum of the van der Waals radii for the interacting atoms. Meanwhile the O1–H1o···N1A bond angles are 153(3)° for **4b**, 155(3)° for **4c** and 153(2)° for **4d**, and all three are directionally positioned also supporting the evidence of hydrogen bonding. Since this interaction is present between H1o and N1A, the angle of the C2–C1–N1A fragment is smaller than C2–C1–N1B in all cases, also indirectly confirming the presence of such bonding; see Table 2 for further details. The C1–C2 bond distance becomes shorter when no hydrogen bonding is present (**4e**) in comparison with **4b**, **4c** and **4d**. The conformational preference observed for the derivatives in the crystallographic phase seemed to be independent of the hydrogen bonding present in three of the four examples, since the N1A–C1–C2–C3 dihedral angles are −37.9(3)° for **4b**, 38.3(3)° for **4c**, 36.5(2)° for **4d** and −40.1(2)° for **4e**. And the corresponding N1B–C1–C2–C3 dihedral angles are 86.9(3)° for **4b**, −85.7(3)° for **4c**, −89.1(2)° for **4d** and 83.2(2)° for **4e**, following the same tendency of orientation of the morpholine rings, with a slight displacement of *ca.* 2–3° in the **4e** derivative. The latter is possibly due to the relaxation of the structure since no hydrogen bonding is present for it. One of the two *tert*-butyl groups of compound **4d** appeared as

Table 1 Collection data and refinement parameters for compounds **4b–e**

Compound	4b	4c	4d	4e
Molecular formula	$C_{15}H_{22}N_2O_3$	$C_{15}H_{21}N_2O_3Br$	$C_{23}H_{38}N_2O_3$	$C_{14}H_{21}N_3O_2$
Molecular weight	278.35	357.25	390.55	263.34
Collection T/K	293(2)	293(2)	293(2)	293(2)
Crystalline system	Orthorhombic	Orthorhombic	Monoclinic	Monoclinic
Space group	P bca	$P\,2(1)2(1)2(1)$	$P\,2(1)/n$	$P\,2(1)/c$
Unit cell dimensions				
$a/Å$	12.2357(12)	7.0621(7)	11.637(8)	15.067(3)
$b/Å$	7.5855(8)	13.9243(14)	10.801(7)	10.150(2)
$c/Å$	31.232(3)	16.4210(16)	19.312(13)	9.665(2)
α (°)	90	90	90	90
β (°)	90	90	103.443(10)	104.544(4)
γ (°)	90	90	90	90
Volume/$Å^3$	2898.8 (5)	1614.8 (3)	2361 (3)	1430.7 (5)
Z	8	4	4	4
ρ (mg m^{-3})	1.276	1.470	1.099	1.223
μ/mm^{-1}	0.089	2.557	0.072	0.083
θ range (°)	1.30 to 25.00	1.92 to 25.00	1.87 to 24.00	1.40 to 24.00
Collected reflections	13325	12635	18617	8409
Ind. reflections [R(int)]	2544 [0.0361]	2838 [0.0354]	3634 [0.0385]	2232 [0.0272]
θ completeness [%]	25.00° [99.9]	25.00° [99.6]	24.00° [98.0]	24.00° [99.6]
Data/Restrictions/Param.	2544/0/185	2838/0/195	3634/55/286	2232/0/172
Goodness-of-fit on F^2	1.268	1.060	1.049	1.125
Final indices [$I > \sigma(I)$] R$_1$	0.0661	0.0266	0.0504	0.0474
Final indices (all data) wR_2	0.1466	0.0664	0.1313	0.1097
$\Delta\rho_{min}$(e Å^3)	-0.208	-0.284	-0.123	-0.106
$\Delta\rho_{max}$(e Å^3)	0.217	0.305	0.127	0.130
Flack parameter	—	–0.012(9)	—	—

a two site rotational disordered moiety and the structure was resolved taking into account this contribution with occupancies of 0.7418 and 0.2582 for each geometrical contribution. The most statistically significant contribution (part A of the disorder) was used for the ellipsoid drawing in Fig. 1.

Acute toxicity test

The *P. phosphoreum* (Microtox™)[30,31] test was developed in order to assess a measurement of toxicity of reported chemicals. The acute toxicity of pipeline protection chemicals to *P. phosphoreum* (*Vibrio fischeri*) was assessed using the Microtox toxicity analyzer. It is worth mentioning that the LBT-Microtox assay has been widely used for lixiviates and residual water solutions for industrial field applications.[32] Microtox Toxicity testing technology is a biosensor-based measurement system for toxicity and provides an effective way to monitor for either accidental or deliberate contamination of water supplies. Any inhibition of normal metabolism, such as that caused by toxicity, results in a decreased rate of luminescence of *Vibrio fischeri*. The higher the level of toxicity, the greater the inhibition of light production results.

In order to visualize the potentiality and robustness of such a test, the *Vibrio fischeri* toxicity of about 1350 organic compounds was determined through the Microtox method,[33] and these data were compared with those obtained from a multitude of other acute toxicity tests on aquatic and terrestrial species, especially the 96 h acute toxicity lethality data of 200 individual chemicals to the fathead minnow (*Pimephales promelas*). A strong correlation was found between the two methods, even though the Microtox tests were carried out with 5 or 15 min of exposure, instead of the normal 96 h exposure time, since this is a very

sensitive microorganism.[23] The results indicated the usefulness of the luminescent bacteria bioassay (Microtox) as a simple and quick method, as well as being cheaper than other methods, but as reliable as many others, and therefore is an alternative to *in vivo* bioassays with higher organisms.[33] Acute toxicity tests performed in several mammalian cell lines are often trackers of such activities.[34] Nevertheless, the latter reviews stated that within this branded Microtox test, plenty of other new protocols have been developed to rank different types of toxicity for pure chemical compounds.[35] These alternative protocols were performed also to reduce or refine some of the mammalian cell procedures with high proficiency in the obtained results, and therefore it has became one of the streamlined tests for this means.

Therefore, the luminescent bacteria toxicity (LBT-Microtox) tests were performed for compounds **4a–h** at 5 and 15 min. and their EC$_{50}$ values were obtained and listed in Table 3. The values for the 5 min Microtox EC$_{50}$ for compounds ranged from 0.080 (**4d**) to 19.80 (**4a**) mg L^{-1}. The less toxic compounds were **4a** (EC$_{50}$ (ppm) 18.30 (33)–19.80 (53)), **4b** (EC$_{50}$ (ppm) 19.30 (44)–18.60 (45)) and **4c** (EC$_{50}$ (ppm) 14.40 (3)–12.20 (7)), which display only slightly toxic values at both 5 and 15 min. The results show that **4a–h** compounds have varying degrees of toxicity, with **4a**, **4b**, **4c**, **4e** and **4f** classified as slightly to moderately toxic agents, **4g** and **4h** as highly toxic chemicals, and **4d** as an extremely toxic compound.

Antibacterial activity against Gram-positive and -negative bacteria

It is well known that certain aerobic as well as anaerobic bacteria, commonly found in the oil and gas operation fields, can generate or influence biocorrosion processes provoking severe damages

Table 2 Selected geometrical parameters for compounds **4b–e**[a,b]

Compound	4b	4c	4d	4e
Bond distance (Å)				
C1–C2	1.529(3)	1.520(3)	1.519(2)	1.516(2)
C1–N1A	1.475(3)	1.478(3)	1.476(2)	1.469(2)
C1–N1B	1.464(3)	1.451(3)	1.458(2)	1.461(2)
N1A$\cdots$N1B	2.407(3)	2.393(3)	2.402(2)	2.394(2)
Bond angle (°)				
N1A–C1–N1B	109.9(2)	109.63(17)	110.00(13)	109.64(13)
C2–C1–N1A[c]	110.7(2)	110.33(18)	110.77(13)	110.64(14)
C2–C1–N1B	114.3(2)	114.26(19)	115.05(13)	113.02(14)
C3–O1–H1o	104(2)	104(3)	103(1)	—
Dihedral angle (°)				
N1A–C1A–C2A–O1A	58.4(3)	60.0(3)	−57.6(2)	59.5(2)
N1A–C4A–C3A–O1A	−59.8(3)	−58.8(3)	59.8(2)	−57.7(2)
N1B–C1B–C2B–O1B	59.1(3)	60.4(3)	57.6(3)	58.4(2)
N1B–C4B–C3B–O1B	−58.7(3)	−57.4(3)	−57.8(3)	−58.2(2)
N1A–C1–C2–C3	−37.9(3)	38.3(3)	36.5(2)	−40.1(2)
N1B–C1–C2–C3	86.9(3)	−85.7(3)	−89.1(2)	83.2(2)
C2–C3–O1–H1o[d]	11(2)	−12(3)	−13(1)	—
Hydrogen bonding				
O1–H1o	0.80(3)	0.72(3)	0.96(2)	—
N1A$\cdots$H1o	1.99(3)	1.99(3)	1.74(2)	—
O1$\cdots$N1A	2.710(3)	2.659(3)	2.640(2)	—
O1–H1o$\cdots$N1A[c]	153(3)	155(3)	153(2)	—
N1A symmetry operation	x, y, z	x, y, z	x, y, z	—

[a] Standard deviation given in parentheses. [b] Numbering according to X-ray structures given in Fig. 1. [c] The hydrogen bonding present is between H1o and N1A, when there is an *ortho* hydroxyl group. Therefore the angle of the C2–C1–N1A fragment is smaller than C2–C1–N1B in all cases, also indirectly confirming the presence of the hydrogen bonding. [d] Dihedral angle of the six-membered ring formed through hydrogen bonding.

Table 3 Acute toxicity of compounds **4a–h**

Compound	EC$_{50}$ 5 min	Toxicity rating[a]	EC$_{50}$ 15 min	Toxicity rating[a]
4a	18.30(33)	Slightly toxic	19.80(56)	Slightly toxic
4b	19.30(44)	Slightly toxic	18.60(45)	Slightly toxic
4c	14.40(3)	Slightly toxic	12.20(7)	Slightly toxic
4d	0.0850(11)	Extremely toxic	0.0800(18)	Extremely toxic
4e	10.88(93)	Slightly toxic	10.88(77)	Slightly toxic
4f	1.02(3)	Moderately toxic	1.02(6)	Moderately toxic
4g	0.61(4)	Highly toxic	0.61(6)	Highly toxic
4h	0.83(5)	Highly toxic	0.68(4)	Highly toxic

[a] Concentration range in ppm, classification, category 5: 0.01–0.10, extremely toxic; 4: 0.1–1.0, highly toxic; 3: 1–10, moderately toxic; 2: 10–100, slightly toxic; 1: 100–1000, particularly nontoxic; and 0: >1000, nontoxic. See ref. 31 and 52 for further details.

in the infrastructure of such installations. These processes begin with the colonization of microorganisms on metallic surfaces of pipelines and equipment. This phenomenon generates a biofilm basically composed of aerobic and anaerobic microbial cells, extracellular polymeric substances, metabolic products, *etc.* The cellular associations formed confer to the present microorganisms the needed protection from the external environment, while their metabolism contributes to the development of the corrosion mechanism itself.

One of the most employed methods to control biocorrosion is chemical treatment based on the use of biocides. Biocides

are active substances that are able to kill microorganisms or to inhibit their growth or reproductive cycle. Not all biocides develop activity against all kinds of microorganisms due to the fact that they can differ in their physical and chemical properties as well as in their efficiency and activity spectrum. The design and selection of an adequate biocide depends on the kind of microorganism, the nature of the material to preserve, the type of corrosion inhibitor used and upon the characteristics of the environment of application.

The strategy to develop the antibacterial assay was to select the compounds with the lowest toxicity, in this case **4a–4c**, and those with the highest, **4d** and **4h**. The latter in order to determine their efficiency and selectivity as ecologic biocides against three different types of aerobic bacteria such as *Escherichia coli*, *Bacillus subtilis* and *Pseudomonas fluorescens*, as well as to investigate if there was any effect of the structural features on these activities. Compounds **4a**, **4b**, **4c** and **4d** showed good activity and exhibited varying degrees of inhibitory effects on bacteria strains (Table 4) and were compared with the *P. phosphoreum* (*Vibrio fischeri*) toxicity levels obtained in the LBT-Microtox assay at 15 min of exposure and described as EC$_{50}$. From the data compiled in Table 4, it can be observed that the biocidal activity of compound **4a** against the *E. coli* bacteria is relatively high with a minimum inhibitory concentration (MIC) of 5 mg L^{-1}, although this activity significantly decreases for *B. subtilis* (75 mg L^{-1}) and *Ps. fluorescens* (25 mg L^{-1}) bacteria, and hence seemed to be bacterioselective in 1 : 5 (*E. coli* : *B. subtilis*) and 1 : 15 (*E. coli* : *Ps. fluorescens*) ratios. On the other hand, compounds **4b** and **4c** showed almost the same bactericidal activity against the three aerobic species within a concentration range of 10 to 15 mg L^{-1}. These results showed that although **4a–c** fall within the same toxicity category, compound **4a** has a marked selectivity to *E. coli* bacteria, while **4b** and **4c** maintain the same biocidal or bactericidal activity to all three aerobic bacteria used. This indicates that small structural changes indeed play different roles in toxicity and also in biocidal activity. In order to visualize the important effects among acute toxicity tests and antibacterial activity, compounds **4a–c** almost preserve the same range of MIC, as shown also for toxicity. Besides, compounds **4d** and **4h** have a very different behaviour, since there are three orders of magnitude among the results obtained for antibacterial activity, *e.g.* 25 or 200 (*E. coli*), 10 or 300 (*B. subtilis*), 15 or 300 (*Ps. fluorescens*) ppm for **4d** or **4h**, against those obtained for acute toxicity (*Vibrio fischeri*) of 0.08 (**4d**) or 0.68 (**4h**) ppm. This again underlines the usefulness of the Microtox assay as a toxicity standard test.

Finally, we can construct a qualitative tendency, according to these results, implying that the molecular design should continue to take into account their efficacy terms; from the latter, we can observe that the substitution at the aromatic ring is a key design since it provides significant differences in the biocidal activity of the resulting chemical. Likewise, the set of compounds provides preliminary information on the relationship between the chemical structure of compounds and their antimicrobial activity.

Theoretical calculations

The structures of compounds **4a–h** were optimized at B3LYP/6-31G(d) level of theory, while single-point calculations were run

Table 4 Inhibition halo [mm] and MIC [ppm] for compounds **4a–d** and **4h** in *B. subtilis*, *E. coli* and *Ps. fluorescens*

Species	Concentration of **4a–d** or **4h**/µg mL^{-1}												MIC	EC$_{50}$[a]
	0	5	10	15	25	50	75	100	200	300	500	1000		
4a (Slightly toxic)														19.8
B. subtilis	0	0	0	0	0	0	15.30(42)	16.11(23)	15.89(93)	(—)	(—)	(—)	75	
E. coli	0	11.90(4)	12.10(12)	12.30(15)	12.60(33)	15.70(65)	18.10(55)	19.13(25)	18.89(54)	(—)	(—)	(—)	5	
Ps. fluorescens	0	0	0	0	15.00(71)	17.50(6)	19.60(88)	18.53(41)	19.11(99)	(—)	(—)	(—)	25	
4b (Slightly toxic)														18.6
B. subtilis	0	0	16.05(65)	18.4(11)	20.55(5)	(—)	(—)	(—)	(—)	(—)	(—)	(—)	10	
E. coli	0	0	13.7(19)	13.0(4)	13.65(5)	(—)	(—)	(—)	(—)	(—)	(—)	(—)	10	
Ps. fluorescens	0	0	13.85(15)	12.9(3)	14.45(5)	(—)	(—)	(—)	(—)	(—)	(—)	(—)	10	
4c (Slightly toxic)														12.2
B. subtilis	0	0	10.1(2)	11.5(5)	13.7(21)	(—)	(—)	(—)	(—)	(—)	(—)	(—)	10	
E. coli	0	0	12.80(1)	11.95(5)	11.9(4)	(—)	(—)	(—)	(—)	(—)	(—)	(—)	10	
Ps. fluorescens	0	0	11.6(3)	11.55(55)	11.3(6)	(—)	(—)	(—)	(—)	(—)	(—)	(—)	10	
4d (Extremely toxic)														0.08
B. subtilis	0	0	11.60(1)	11.75(1)	11.70(1)	(—)	(—)	(—)	(—)	(—)	(—)	(—)	10	
E. coli	0	0	12.15(5)	11.75(15)	12.05(5)	(—)	(—)	(—)	(—)	(—)	(—)	(—)	10	
Ps. fluorescens	0	0	32.0(18)	32.5(15)	33.25(25)	(—)	(—)	(—)	(—)	(—)	(—)	(—)	10	
4h (Highly toxic)														0.68
B. subtilis	0	0	0	0	0	0	0	0	0	7.4(5)	17.33(20)	19.98(55)	300	
E. coli	0	0	0	0	0	0	0	0	7.13(40)	7.5(4)	6.77(17)	18.41(25)	200	
Ps. fluorescens	0	0	0	0	0	0	0	0	0	7.15(15)	15.58(2)	19.0(43)	300	

"0" denotes no inhibition zone formation. (—) indicates that there is no data available at those concentrations due to the findings of MIC. For *B. subtilis*, *E. coli*, and *Ps. fluorescens*, the diameter of the inhibition zone [mm] was measured after 16 h of incubation at 30 °C. [a] EC$_{50}$ (in ppm) values at 15 min are placed herein to compare toxicity and batericidal activity.

Table 5 Energy values of biocide compounds **4a–h** obtained at B3LYP/6-311G(d) level of theory

Compound	Energy (hartrees)
4a	−613.8341789
4b	−920.175673
4c	−3493.719691
4d	−1234.744319
4e	−860.9747614
4f	−962.9006274
4g	−998.5926152
4h	−1228.515639

Table 6 Dihedral angles of the six-membered rings formed through hydrogen bonding[a] in compounds **4b–d** obtained at B3LYP/6-31G(d) level of theory

Dihedral angle	**4b**	**4c**	**4d**
N4-C5-C6-C7	−37.64	−37.22	−38.86
C5-C6-C7-O7	6.23	6.25	6.21
C6-C7-O7-H7o	9.55	9.56	10.68
C7-O7-H7o-N4	10.02	9.58	9.04
O7-H7o-N4-C5	−38.28	−37.63	−38.36
H7o-N4-C5-C6	37.80	37.35	38.54

[a] The numbering of the selected dihedral angles is in accordance with that given in Scheme 1b.

at B3LYP/6-311G(d) level of theory, for energy measurement means. In Tables 5 and 6 are listed the energy values and selected dihedral angle parameters of hydrogen bonding in compounds **4b**, **4c** and **4d**, respectively (see Scheme 1b for numbering). Compound **4a** shows two symmetry planes: the first one through the H-C5-H atoms and the second one though O1-N4-C5-N4′-O1′, and one C_2 axis through the C5 atom.

Regarding to the morpholine cycle, a chair conformation is observed for all compounds. The aromatic ring, mainly the C6–C7 bond, is not parallel to the C5–H5 bond. Thus, the dihedral angle value of the H5-C5-C6-C7 fragment for **4b–h** is 25.98°, 26.58°, 24.64°, 14.21°, 17.94°, 17.91°, −54.42°, respectively. Hence, a substituent in the *ortho* position with respect to the C6 atom induced an increase in the dihedral angle value, and it is higher if the group is bulky as in **4h**. Clearly, the hydrogen of the C5 atom shows an *anti* relation with: the O7-H7o group of **4b**, **4c**, and **4d**, with the H(C11) atom in **4g** and **4h**. In the case of compound **4e**, the nitrogen atom shows a *syn* relationship

with the H5(C5) atom, with a dihedral angle for the H5-C5-C6-N7 fragment of 23.22°. This structure is in accordance with the X-ray diffraction. Furthermore, the energy of **4e**, with *anti* relationship, is 1.48 kcal mol^{-1} less stable that the *syn* structure.

In compounds **4b**, **4c**, and **4d**, which have an OH (numbered O7-H7o as in Scheme 1b) group at C7, there are hydrogen bonds in the crystal phase with the N4 atom, generating a six-membered cycle where the N4···H7o theoretical distance is 1.78, 2.41, and 1.75 Å, respectively. The dihedral angles of this six-membered ring are listed in Table 6, and the numbering employed is that of Scheme 1b. The Laplacian values for the hydrogen bonding in **4b**, **4c** and **4d** were 0.1153, 0.1152, and 0.1274. Also in compound **4h** is observed a weak hydrogen bonding between the N4 and H(C21) atoms; in this case the bonding distance is 2.31 Å, whereas the Laplacian value was 0.0664.

Table 7 ^{13}C chemical shifts (ppm) of compounds **4a–h** obtained at B3LYP/6-31G(d) level of theory

Compound	Experimental	Theoretical
4a	81.5	82.63
4b	89.6	87.57
4c	88.9	87.63
4d	90.4	95.79
4e	89.4	91.68
4f	88.8	90.18
4g	84.5	83.88
4h	84.1	87.76

The ^{13}C NMR shielding tensors for all compounds were calculated by using the GIAO methodology[36–39] at the B3LYP/6-31G(d) level. The isotropic shielding values were used to calculate the chemical shifts (δ) with respect to TMS. The absolute $\sigma(^{13}$C) of 184.1 ppm reported by Jameson and Jameson was employed to obtain the calculated shift.[40] The calculated and experimental ^{13}C NMR chemical shifts (δ^{13}C) for the C5 atom are listed in Table 7; the calculated values show a good correlation with the experimental values, even though for **4e** the difference is 5.32 ppm, which could be acceptable taking into account the fact that the calculations were carried out in the gas phase.

Quantitative structure activity relationships (QSAR)

The molecular design and physicochemical properties of compounds **4a–h** were related and discussed through a QSAR study in order to understand the ruling variables in the chemical structure that give varying degrees of biological activities. Through the quantum-chemical parameters calculated for these molecules and discussed in the last section, the construction of a linear multivariate model was selected. An exhaustive statistical search of chosen molecular descriptors within the proposed linear multivariate model, starting from one to six, was carried out through least squares in order to relate them to their acute toxicity and understand the obtained trend. Since the behaviour of organic compounds is related to the inherent properties of the molecular structure under study, this can be correlated, not only with physicochemical properties, but also to the most difficult industrial or biological responses, *e.g.* environmental partitioning and transport processes between different phases, as well as unwanted toxicological responses in organisms. For approximately 150 years, scientists have been

investigating this phenomenon to achieve quantitative correlations and therefore to understand relations among molecular structure and their properties/activities.[41,42] In general, models for estimating key fate parameters and toxicological responses have settled on three sets of molecular properties governing activity, *i.e.*, hydrophobic, electronic and inherent structural features of the tested compounds. The hydrophobicity is related to the individual compound affinity for partitioning between aqueous and hydrophobic (abiotic or biotic) phases, *e.g.* a biological membrane. The inherent structural and electronic molecular properties (molecular orbitals and their analysis) have been related to the ability to, for example, pass through the membrane, and bind to a receptor or specific sorption or binding site.[43,44]

Therefore we consider that the important molecular features for a feasible QSAR model related to toxicity have been constructed by considering the following parameters: the highest occupied molecular orbital energy (E_{HOMO}), the lowest unoccupied molecular orbital energy (E_{LUMO}), absolute value of the difference of the frontier molecular orbitals (GAP [=] $|E_{\mathrm{LUMO}} - E_{\mathrm{HOMO}}|$), Mulliken atomic charge (AC_{MK}), atomic charge of NBO (AC_{NBO}), dipole moment (μ), the hydrophobicity considered by the logarithm of n-octanol/water partition coefficient (log P), molecular volume (Vol), electrostatic potential (ESP), and δ^{13}C. The ACs, the ESP, and the δ^{13}C were selected for the atom placed at position 5 (C5) since it is conserved among the whole series and due to its chemical position is sensitive to substitutions in the molecule, as in **4a–h**. In Table 8 are listed the values for all these chosen chemical indexes. The least square runs taken into account were those with a value of more than 0.9 of the obtained adjusted correlation coefficient (R^2_{adj}). In Table 9 are listed the runs that achieved this. Of these preselected 27 runs, the 11th, 18th, 19th, 20th, 22nd, 23rd, 24th, 25th, 26th, and 27th gave an R^2_{adj} value higher than 0.98. Furthermore, any energy value of frontier orbitals (E_{HOMO} or E_{LUMO}), or the GAP is contained in them.

Thus, considering the F value of the runs with $R^2_{\mathrm{adj}} > 0.98$, entry 18 gave the best correlation for this system; however, if only the R^2_{adj} value is taken into account, the other runs gave also a good correlation. In this way, equations 1–3, presented in Table 10, show the coefficients for the 18th, 23rd and 27th entries of Table 9, respectively (runs with an F value >1000). It is important to underline that for these runs, the log P and δ^{13}C are considered, and at first sight the former is independent of the conformation, whereas the latter depends on the chemical

Table 8 Parameters for biocide compounds **4a–h** obtained at B3LYP/6-31G(d) level of theory

Compound	E_{HOMO}	E_{LUMO}	$|\mathrm{GAP}|$	AC_{MK}	AC_{NBO}	μ	log P^a	Volume	ESP	δ^{13}C
4a	−0.20150	0.03142	0.23292	−0.9841	0.0395	1.6148	−0.18	177.157	−14.7233	81.5
4b	−0.01418	0.00323	0.01741	−0.6422	0.1886	1.9442	1.28	204.609	−14.6950	89.6
4c	−0.00599	0.02156	0.02755	−0.7481	0.1891	2.4016	2.07	233.012	−14.6870	88.9
4d	−0.01066	0.0033	0.01396	−0.5972	0.1348	1.9868	4.54	302.489	−14.6958	90.4
4e	−0.02688	0.03265	0.05953	−1.1669	0.1813	3.1952	1.12	233.777	−14.7086	89.4
4f	−0.01124	0.03532	0.04656	−0.6042	0.1945	1.6607	2.76	245.519	−14.7089	88.8
4g	−0.02149	0.01488	0.03637	−0.3103	0.1891	1.0655	2.57	216.622	−14.7042	84.5
4h	−0.01341	0.00662	0.02003	−0.0606	0.1294	1.3661	3.89	298.277	−14.7016	84.1

E in hartrees; μ in debye; Volume in cm^3 per molecule; δ^{13}C in ppm. ^{a} This descriptor was calculated at the NDDO-PM3 level of theory due to parametrization needs for it.

Table 9 Statistical R^2, R^2_{adj}, and F values for runs containing 3 to 6 molecular descriptors

Run	Molecular descriptor set	R^2	R^2_{adj}	F
1	AC_{NBO}, log P, ESP	0.9540	0.9195	27.665
2	AC_{NBO}, log P, Vol, ESP	0.9581	0.9023	17.168
3	GAP, AC_{NBO}, log P, $\delta^{13}C$	0.9775	0.9475	32.556
4	E_{LUMO}, AC_{NBO}, μ, log P, ESP	0.9722	0.9027	13.992
5	E_{LUMO}, AC_{NBO}, log P, Vol, ESP	0.9732	0.9062	14.529
6	GAP, AC_{NBO}, μ, log P, ESP	0.9722	0.9029	14.011
7	GAP, AC_{NBO}, log P, Vol, ESP	0.9717	0.9009	13.725
8	E_{HOMO}, E_{LUMO}, AC_{NBO}, log P, $\delta^{13}C$	0.9776	0.9216	17.466
9	E_{LUMO}, AC_{MK}, μ, log P, $\delta^{13}C$	0.9768	0.9188	16.830
10	E_{LUMO}, μ, log P, ESP, $\delta^{13}C$	0.9775	0.9213	17.398
11	E_{LUMO}, log P, Vol, ESP, $\delta^{13}C$	0.9923	0.9923	180.988
12	GAP, AC_{NBO}, μ, log P, $\delta^{13}C$	0.9781	0.9235	17.901
13	E_{LUMO}, AC_{MK}, μ, log P, Vol, ESP	0.9948	0.9634	31.732
14	E_{HOMO}, E_{LUMO}, AC_{MK}, μ, log P, $\delta^{13}C$	0.9874	0.9116	13.024
15	E_{HOMO}, E_{LUMO}, AC_{MK}, μ, Vol, $\delta^{13}C$	0.9932	0.9526	24.436
16	E_{HOMO}, E_{LUMO}, AC_{NBO}, μ, Vol, $\delta^{13}C$	0.9878	0.9148	13.522
17	E_{HOMO}, E_{LUMO}, AC_{NBO}, log P, Vol, $\delta^{13}C$	0.9880	0.9162	13.759
18	E_{HOMO}, E_{LUMO}, AC_{NBO}, log P, ESP, $\delta^{13}C$	0.9999	0.9999	10162.335
19	E_{LUMO}, E_{LUMO}, log P, Vol, ESP, $\delta^{13}C$	0.9984	0.9889	104.486
20	E_{HOMO}, AC_{NBO}, μ, log P, Vol, $\delta^{13}C$	0.9973	0.9808	60.442
21	E_{HOMO}, AC_{NBO}, μ, log P, ESP, $\delta^{13}C$	0.9902	0.9315	16.869
22	E_{LUMO}, AC_{MK}, μ, log P, Vol, $\delta^{13}C$	0.9992	0.9941	196.054
23	E_{LUMO}, AC_{MK}, μ, log P, ESP, $\delta^{13}C$	0.9991	0.9941	1805.727
24	E_{LUMO}, AC_{MK}, log P, Vol, ESP, $\delta^{13}C$	0.9986	0.9941	118.942
25	E_{LUMO}, μ, log P, Vol, ESP, $\delta^{13}C$	0.9984	0.9890	106.025
26	GAP, AC_{NBO}, μ, log P, Vol, $\delta^{13}C$	0.9997	0.9979	551.384
27	GAP, AC_{NBO}, log P, Vol, ESP, $\delta^{13}C$	0.9999	0.9995	2401.463

Table 11 Experimental and calculated EC_{50} (ppm) for equations 1, 2 and 3 as obtained in runs 18, 23 and 27

Compound	EC_{50} (exp.)	EC_{50} (18)	EC_{50} (23)	EC_{50} (27)
4a	19.8	19.7576	19.8250	19.8434
4b	18.6	18.5430	18.4413	18.6357
4c	12.2	12.1463	12.2483	12.2246
4d	0.08	0.0878	0.0622	0.2426
4e	10.88	10.8840	10.8511	11.0148
4f	1.02	0.9865	1.0362	1.1193
4g	0.61	0.5365	0.4481	0.5930
4h	0.68	0.5916	0.6764	0.6450

Fig. 2 Plot of the correlation between experimental and calculated EC_{50}.
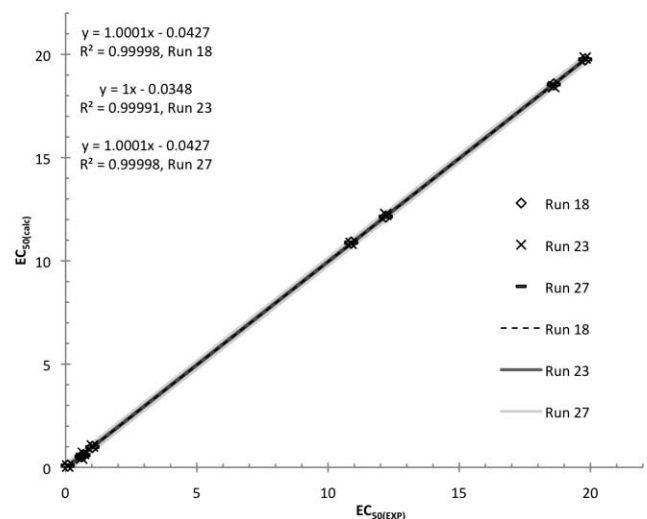
environment at the molecule. Therefore, these values are very important to consider for the QSAR analysis. As observed for many other QSAR/QSPR analysis,[25] in the present work the log P value stands out again as the universal chemical descriptor. In Table 11 and Fig. 2 are reported and plotted the experimental *vs.* theoretical EC_{50} values, showing that between run 18 and run 27 there are no significant statistical differences, according to the difference between experimental and theoretical results and their plots. Thus, both models are equally efficient for the description of the chemical system, this in order to modulate the biological effect, *e.g.* toxicity. Finally, this analysis allowed the fine-tuning of the chemical structure in order to choose the best prototype of an ecological biocide. The phenol-bearing structures (**4b**, **4c** and **4d**, derived from salicylidenes) are best tuned within these variables since the substitution in the phenol fragment governs both the toxicity and the biocidal potency, affecting in a wide interval the log P, the ESP and the $\delta^{13}C$ descriptors. A more hydrophobic substitution (**4d**) extremely increases the toxicity, ruling out its application as a biocide. In contrast to this trend, the lead compound, the **4a** derivative, and two of the more hydrophobic compounds, **4b** and **4c**, are the best candidates because diminished toxicity and preserved biocidal potency were obtained at the same time. Among these chosen three, the latter two were selected to be tested as prototype biocides in further

pilot scale experiments (under progress), since the salicyliden (acetylsalicylic acid analogue) fragments are well known to have a variety of beneficial effects in higher organisms[45–47] but protective against other harmful lower organisms.[48–51]

Conclusions

The results presented herein show that it is possible to find a quantitative correlation between the molecular structure and toxicity of the synthesized compounds **4a–h**. This was accomplished through a QSAR study which implied the calculation of molecular indexes or descriptors based on rigorous enough computational methods. Likewise, it was observed that the ^{13}C NMR chemical shift of the bridge methinic group plays a significant role within the correlation study. This is mainly due to the different chemical environments or substituents that were introduced in the design of the studied compounds.

Toxicity results indicate that three of the synthesized compounds (**4a**, **4b** and **4c**) would be considered as non-toxic chemicals based on the European Union criteria[52] for the classification

Table 10 Equations for runs 18, 23, and 27

Run	Equation	Eq. No.
18	$EC_{50} = 3677.487 + 169.124(E_{HOMO}) - 137.026(E_{LUMO}) - 147.777(AC_{NBO}) - 9.737(\log P) + 240.515(ESP) - 0.909(\delta^{13}C)$	(1)
23	$EC_{50} = 3076.187 - 246.296(E_{LUMO}) + 17.568(AC_{MK}) + 9.216(\mu) - 8.226(\log P) + 199.437(ESP) - 1.366(\delta^{13}C)$	(2)
27	$EC_{50} = 3753.911 - 150.283(GAP) - 130.164(AC_{NBO}) - 9.779(\log P) + 0.013(Vol) + 246.189(ESP) - 0.899(\delta^{13}C)$	(3)

of dangerous substances, while their biocidal activity is still high enough against different harmful microorganisms. These results also show that there is an important effect of the substituent directly bonded to the methinic group on the biocidal selectivity of such compounds against different kinds of microorganisms.

In summary, this piece of work shows that it is possible to modulate the toxicity of these kinds of compounds through the correlation of some chosen molecular and experimental indices in order to make them selective as biocides. And concomitantly, the can be selective to certain kinds of harmful microorganisms present in the chemical environments of the petroleum industry.

These and other efforts feed the necessary knowledge in the area of rational design of green molecules for biological applications. These approaches, nowadays and in the future, stand as a key role of chemical areas to preserve good environmental conditions, not only in water but also in any media where human incursion has been present and ecological aid is needed.

Experimental

Paraformaldehyde (**1a**), aromatic aldehydes (**2b–h**) and morpholine (**3**) were purchased from Aldrich Co. All reactions and operations were carried out under atmospheric conditions.

Instrumentation

NMR experiments were performed on a VARIAN Mercury 200-BB spectrometer. The ^{1}H and ^{13}C chemical shifts [ppm] are relative to internal SiMe$_4$ (TMS). Coupling constants are quoted in Hz. The IR spectra were recorded in the range of 4000 and 400 cm^{-1} on a Bruker Tensor-27 FT-IR spectrometer, using KBr pellets, or the ATR technique. The X-ray structure determination was performed on a BRUKER-AXS APEX diffractometer with a CCD area detector ($\lambda_{\text{Mo-K}\alpha}$ = 0.71073 Å, monochromator: graphite). All determinations were carried out at atmospheric conditions and at room temperature (20 °C).

General method for the preparation of compounds 4a–h

The synthesis from aldehydes (**1a, 2b–h**) with morpholine (**3**) using 600 W of microwave irradiation power, setup temperature of 100 °C, over a period of 10 min led to eight new 4,4′-dimorpholyl-methanes (**4a–h**) with good yields (65 to 98%). A general case is herein described for compound **4b** and the same molar ratios were applied for all the **4** series. The quantity of 2 g of salicylaldehyde (**2b**, 16.38 mmol) was mixed with 2.85 g of morpholine (**3**, 32.76 mmol) to load a 1 : 2 stoichiometric ratio to the reactor. This mixture was exposed to microwave irradiation under continuous stirring. After the first 5 min of irradiation, the reaction was stopped and its course was monitored with FT-IR and ^{1}H NMR showing a remnant characteristic band (FT-IR) or signal (NMR) of the CHO group of **2b**. Another exposition period of 5 min accomplished the reaction, since the corresponding signal and band of the aldehyde precursor were absent at this stage. This procedure yields 4.33 g of compound **4b** (95%). The ^{1}H NMR confirmed the purity of the product, since the spectra of the reaction crude only showed the signals of **4b**.

Characterization and spectroscopic data

Dimorpholinomethane (4a). Yield 98%, IR (cm^{-1}): 2958, 2851, 2796, 1653, 1456, 1414, 1356, 1331, 1151, 1113, 1034, 1017, 866. ^{1}H NMR (CDCl$_3$), 200 MHz, δ (ppm): 3.69 (dd, J = 4.8, 4.6, 8H, *H2*), 2.91 (s, 1H, *H5*), 2.50 (t, J = 4.6, 8H, *H3*). ^{13}C NMR (CDCl$_3$), 50 MHz, δ (ppm): 81.5 (1C, *C5*), 66.8 (4C, *C2*), 51.8 (4C, *C3*). Elemental analysis calculated (%) for C$_9$H$_{18}$N$_2$O$_2$: C, 58.04; H, 9.74; N, 15.04; found: C, 57.93; H, 9.65; N, 14.98.

2-(Dimorpholinomethyl)phenol (4b). Yield 95%, IR (cm^{-1}): 3435, 2922, 2825, 1655, 1578, 1435, 1414, 1346, 1319, 1141, 1118, 1015, 874. ^{1}H NMR (CDCl$_3$), 200 MHz, δ (ppm): 7.22 (ddd, Jo=6.2, 5.7, Jm=2.1, 1H, *H9*), 6.86(dd, Jo=5.2, Jm=2.1, 1H, *H11*), 6.84 (ddd, Jo=6.2, 5.2, Jm=2.6, 1H, *H10*), 6.83 (dd, Jo=5.7, Jm=2.6, 1H, *H8*), 3.77 (s, 1H, *H5*), 3.72 (dd, J = 4.8, 4.4, 8H, *H2*), 2.58 (dd, J = 4.8, 4.4, 8H, *H3*). ^{13}C NMR (CDCl$_3$), 50 MHz, δ (ppm): 157.0 (1C, *C7*), 130.1 (1C, *C11*), 129.5 (1C, *C9*), 118.9 (1C, *C10*), 117.1 (1C, *C6*), 116.3 (1C, *C8*), 89.6 (1C, *C5*), 66.9 (4C, *C2*), 49.5 (4C, *C3*). Elemental analysis calculated (%) for C$_{15}$H$_{22}$N$_2$O$_3$: C, 64.73; H, 7.97; N, 10.06; found: C, 64.23; H, 7.86; N, 10.01. Suitable crystals for the X-ray diffraction were obtained from the dissolution of 0.5 g of **4b** in 15 mL of a 7 : 3 chloroform : hexanes mixture after one week of slow evaporation of the solution.

4-Bromo-2-(dimorpholinomethyl)phenol (4c). Yield 94%, IR (cm^{-1}): 3449, 2982, 2961, 1603, 1578, 1452, 1366, 1346, 1192, 1161, 1068, 1015, 874. ^{1}H NMR (CDCl$_3$), 200 MHz, δ (ppm): 7.31 (dd, Jo=8.7, Jm= 2.4, 1H, *H9*), 6.97 (d, Jm=2.4, 1H, *H11*), 6.72 (d, Jo=8.7, 1H, *H8*), 3.72 (s, 1H, *H5*), 3.71 (dd, J = 4.6, 4.4, 8H, *H2*), 2.56 (dd, J = 4.6, 4.4, 8H, *H3*). ^{13}C NMR (CDCl$_3$), 50 MHz, δ (ppm): 156.2 (1C, *C7*), 132.2, 132.1 (2C, *C9, C11*, maybe interchanged), 119.1 (1C, *C6*), 118.3 (1C, *C8*), 110.7 (1C, *C10*), 88.9 (1C, *C5*), 66.7 (4C, *C2*), 49.4 (4C, *C3*). Elemental analysis calculated (%) for C$_{15}$H$_{21}$BrN$_2$O$_3$: C, 50.43; H, 5.93; N, 7.84; found: C, 50.24; H, 5.82; N, 7.81. Suitable crystals for X-ray diffraction were obtained from the dissolution of 0.8 g of **4c** in 20 mL, 6 : 4 chloroform : hexanes mixture, after 10 days of slow evaporation of the solution.

2,4-Di-*tert*-butyl-6-(dimorpholinomethyl)phenol (4d). Yield 88%, IR (cm^{-1}): 3476, 2961, 2855, 1650, 1482, 1454, 1361, 1323, 1159, 1119, 1071, 1016, 870. ^{1}H NMR (CDCl$_3$), 200 MHz, δ (ppm): 7.22 (d, Jm= 2.4, 1H, *H9*), 6.63 (d, Jm=2.4, 1H, *H11*), 3.75 (s, 1H, *H5*), 3.72 (dd, J = 4.6, 4.0, 8H, *H2*), 2.59 (dd, J = 4.6, 4.0, 8H, *H3*), 1.39 (s, 9H, *H12a,b,c*), 1.28 (s, 9H, *H13a,b,c*). ^{13}C NMR (CDCl$_3$), 50 MHz, δ (ppm): 153.3 (1C, *C7*), 139.9 (1C, *C10*), 135.4 (1C, *C8*), 124.7 (1C, *C11*), 123.2 (1C, *C9*), 115.7 (1C, *C6*), 90.4 (1C, *C5*), 67.0 (4C, *C2*), 49.4 (4C, *C3*), 34.7 (1C, *C12*), 34.0 (1C, *C13*), 31.6 (3C, *C13 a, b, c*), 29.4 (3C, *C12 a, b, c*). Elemental analysis calculated (%) for C$_{23}$H$_{38}$N$_2$O$_3$: C, 70.73; H, 9.81; N, 7.17; found: C, 70.61; H, 9.75; N, 7.11. Suitable crystals for X-ray diffraction were obtained from the dissolution of 0.4 g of **4d** in a 20 mL, 5 : 5 chloroform : hexanes mixture after 25 days of slow evaporation of the solution.

4,4′-(Pyridin-2-ylmethylene)dimorpholine (4e). Yield 89%, IR (cm^{-1}): 3374, 2964, 2825, 1632, 1592, 1454, 1436, 1328, 1331, 1109, 1069, 1018, 861. ^{1}H NMR (CDCl$_3$), 200 MHz, δ (ppm): 8.61 (dd, Jo= 5.0, Jm= 1.7, 1H, *H8*), 7.70 (ddd, Jo= 7.9, 7.5,

Jm= 1.7, 1H, *H10*), 7.30 (dd, Jo= 7.9, Jm= 1.2, 1H, *H11*), 7.22 (ddd, Jo= 7.5, 5.0, Jm= 1.2, 1H, *H9*), 3.88 (s, 1H, *H5*), 3.68 (dd, $J = 4.7, 4.3, 8H, H2$), 2.55 (dt, $J = 11.9, 4.3, 4H, H3ec$), 2.44 (dt, $J = 11.9, 4.3, 4H, H3ax$). ^{13}C NMR (CDCl$_3$), 50 MHz, δ (ppm): 154.9 (1C, *C6*), 148.8 (1C, *C8*), 135.4 (1C, *C10*), 122.8, 122.6 (2C, C9, *C11*), 89.4 (1C, *C5*), 66.9 (4C, *C2*), 49.3 (4C, *C3*). Elemental analysis calculated (%) for C$_{14}$H$_{21}$N$_3$O$_2$: C, 63.85; H, 8.04; N, 15.96; found: C, 63.45; H, 8.01; N, 15.43. Suitable crystals for the X-ray diffraction were obtained from the dissolution of 1.0 g of **4e** in a 40 mL, 85 : 15 chloroform : hexanes mixture after 20 days of slow evaporation of the solution.

4,4′-((4-Isopropylphenyl)methylene)dimorpholine (4f). Yield 90%, IR (cm^{-1}): 2957, 2849, 1642, 1507, 1453, 1345, 1328, 1111, 1017, 1034, 877. ^{1}H NMR (CDCl$_3$), 200 MHz, δ (ppm): 7.17 (d, Jo= 8.2, 2H, H8, *H10*), 7.11 (d, Jo= 8.2, 2H, *H7, H11*), 3.67 (t, $J = 4.4, 8H, H2$), 3.61 (s, 1H, *H5*), 2.90 (hep, $J = 7.0$, 1H, *H12*), 2.43 (t, Jo= 4.4, 8H, *H3*), 1.25 (d, $J = 7.0$, 6H, *H12a,b*). ^{13}C NMR (CDCl$_3$), 50 MHz, δ (ppm): 148.3 (1C, *C9*), 131.3 (1C, *C6*), 128.7 (2C, *C8, C10*), 125.7 (2C, *C7, C11*), 88.8 (1C, *C5*), 67.2 (4C, *C2*), 49.5 (4C, *C3*), 33.7 (1C, *C12*), 24.0 (2C, *C12a,b*). Elemental analysis calculated (%) for C$_{18}$H$_{28}$N$_2$O$_2$: C, 71.02; H, 9.27; N, 9.20; found: C, 70.97; H, 9.16; N, 9.02.

4,4′-(Naphthalen-1-ylmethylene)dimorpholine (4g). Yield 73%, IR (cm^{-1}): 2954, 2853, 1656, 1594, 1453, 1366, 1346, 1137, 1116, 1014, 865. ^{1}H NMR (CDCl$_3$), 200 MHz, δ (ppm): 8.50 (bs, 1H, *naph*), 7.88-7.78 (m, 2H, *naph*), 7.51-7.24 (m, 4H, *naph*), 4.60 (bs, 1H, *H5*), 3.69 (dd, $J = 4.8, 4.6, 8H, H2$), 2.59 (dt, $J = 11.8, 4.6, 4H, H3ec$), 2.48 (dt, $J = 11.8, 4.8, 4H, H3ax$). ^{13}C NMR (CDCl$_3$), 50 MHz, δ (ppm): 133.8, 133.0, 130.0 (Cq, 3C, *naph*), 128.7, 128.1, 127.1, 125.5, 125.1, 124.5, 124.0 (Ct, bs, 7C, *naph*), 84.5 (bs, 1C, *C5*), 67.1 (4C, *C2*), 49.8 (4C, *C3*). Elemental analysis calculated (%) for C$_{19}$H$_{24}$N$_2$O$_2$: C, 73.05; H, 7.74; N, 8.97; found: C, 72.96; H, 7.61; N, 8.78.

4,4′-(Pyren-1-ylmethylene)dimorpholine (4h). Yield 65%, IR (cm^{-1}): 3039, 2950, 2841, 1678, 1595, 1454, 1373, 1137, 1112, 1061, 1016, 843. ^{1}H NMR (CDCl$_3$), 200 MHz, δ (ppm): 9.40 (m, 1H, *pyren*), 8.43-7.97(m, 8H, *pyren*) 4.91 (bs, 1H, *H5*), 3.71 (dd, $J = 4.8, 4.4, 8H, H2$), 2.62 (dt, $J = 11.8, 4.6, 4H, H3ec$), 2.54 (dt, $J = 11.8, 4.8, 4H, H3ax$). ^{13}C NMR (CDCl$_3$), 50 MHz, δ (ppm): 131.3, 130.7 (Ct, 2C, *pyren*), 130.6 (Cq, 1C, *pyren*), 127.4, 17.3, 127.2 (Cq, 3C, *pyren*), 127.0, 126.9 (Ct, 2C, *pyren*), 126.7, 126.4 (Cq, 2C, *pyren*), 125.9, 125.2, 124.8 (Ct, 3C, *pyren*), 124.4 (Cq, 1C, *pyren*), 124.1, 122.8 (Ct, 2C, *pyren*), 84.1 (bs, 1C, *C5*), 67.2 (4C, *C2*), 49.9 (4C, *C3*). Elemental analysis calculated (%) for C$_{25}$H$_{26}$N$_2$O$_2$: 77.69; H, 6.78; N, 7.25; found: C, 77.53; H, 6.61; N, 7.15.

X-Ray crystallography

The X-ray diffraction study of **4d**, **4c**, **4d** and **4e** was carried out on a BRUKER-AXS APEX diffractometer with a CCD area detector (Mo-Kα= 0.71073 Å, monochromator: graphite). Frames were collected at $T = 100$ K or 298 K *via* ω- and θ-rotation at 10 s per frame.[53] The measured intensities were reduced to F2 and corrected for absorption with SADABS (SAINT+NT[54]). Structure solution, refinement, and data output were carried out with the SHELXTL-NT,[55] SHELXS-97,[56] and SHELXL-97[56] programs. Non-hydrogen atoms were refined anisotropically. All

data were corrected for Lorentz and polarization effects. All additional treatments were done through the WIN-GX program set,[57] some selected geometrical treatments and measurements were performed with the PARST[58] utility; the corresponding molecular graphs were prepared with ORTEP 3 program.[59]

Computational procedure

The DFT calculations, implemented in the Gaussian 98 software,[60] were done at B3LYP/6-31G(d)//B3LYP/6-311G(d) level. This functional[25,26] has the form: $A*E_X^{Slater} + (1\text{-}A)*E_X^{HF} + B*\Delta E_X^{Becke} + E_C^{VWN} + C*\Delta E_C^{non\text{-}local}$,[61–64] where the non-local correlation is provided by the LYP expression, and VWN is the Vosko, Wilk, and Nusair correlation functional, which fits the RPA solution to the uniform gas, often referred to as local spin density (LSD) correlation. The VWN is used to provide the excess local correlation required, since LYP contains a local term essentially equivalent to VWN. Zero-point energy corrections (ZPE) were done for all the calculations. The ^{13}C NMR shielding tensors were calculated employing the Gauge Independent Atomic Orbitals (GIAO)[36–39] at B3LYP/6-31G(d) level. The isotropic shielding values have been defined as $\sigma_{iso} = 1/3(\sigma_{11} + \sigma_{22} + \sigma_{33})$, being σ_{ii} the principal tensor components, that were used to calculate the isotropic chemical shifts δ with respect to TMS ($\delta^X = \sigma^{TMS} - \sigma^X$).[40,65,66] Electrostatic potential (ESP)-fitting charges, were derived from the DFT-calculated molecular electrostatic potential distribution using the Merz-Singh-Kollman (MK) method. Natural bond orbital (NBO)[67–69] was performed with NBO 5.0 program implemented in Gaussian 98. Finally, the parameters for the QSAR study were obtained at B3LYP/6-311G(*d*) level. The hydrophobic parameter as partition coefficient (log *P*) was calculated by HyperChem 8.0 software.

Acute toxicity LBT-microtox test

Herein, the LBT-Microtox tests[30,31] for specific acute toxicity measurements were carried out to select the most environmentally benign compound as a biocide prototype. All compounds were tested in triplicate, in these tests a vial with bacteria was reconstituted in 1 mL of solution and maintained at 3 °C in an incubator well in the analyzer. For each test, a serial dilution of the compounds was prepared in 2% saline water. In addition, a series of saline solutions containing 10^6 colony units of *P. phosphoreum* was prepared in glass cuvettes by pipetting 10 μL of the reconstituted bacterial suspension into 500 μL of a 2% saline solution. These solutions were incubated in temperature-controlled wells (6 °C) during 15 min. and measured. The activity of the treated compounds was recorded after 5 and 15 min. of exposure to the tested chemical. The results of the Microtox test are expressed in terms of the EC$_{50}$. Each test cuvette contains roughly a million of individual test organisms that are exposed to the chemical. The system automatically measures a single parameter, the simultaneous light output of all of the organisms at different concentrations and by triplicate and performs the statistical obtaining of the effective concentration to determine a 50 percent loss of light in the test bacteria (EC$_{50}$). The luminometer and supporting computer software (MicrotoxOmni® software) with a standard log-linear model are used to determine the EC$_{50}$ value. All EC$_{50}$ values are

expressed as weight or percent per mL with 95% confidence intervals and reported as the mean of three pseudoreplicates or true replicates; replicates are a statistical measurement of the test's precision. The lower the EC_{50} value the greater the toxicity of the sample.[32]

Determination of the antibacterial activity against Gram-positive and -negative bacteria

Tested compounds were **4a–4e** and **4h**, achieved through an antibacterial assay using the agar-well diffusion method.[4] Flat-bottomed, 90 mm Petri dishes were used. Seeding agar was prepared by cooling TSA medium to 40 °C and then adding the required amount of bacterial suspension (8×10^8 bacteria per 100 mL). Four wells per dish were dug in the medium with the help of a sterile metallic borer with centres of at least 24 mm. Each compound was dissolved in water at concentrations of 10^{-3}, 10^{-2}, 1.0, 2.5, 5, 10, 25, 50, 75, and 100 µg mL^{-1}. Samples of 50 µL for each dilution were applied in duplicate into the corresponding wells. Afterwards, the Petri dishes were cooled at 4 °C for 60 min to allow a complete diffusion of the compounds through the medium. Water controls were also included in these assays. Petri dishes were then incubated at a suitable growth temperature for the bacteria (30 °C ± 2) for 16 h. The inhibition zone of the bacterial growth, formed around each slot, was measured in millimetres. Standard deviation was under 5% in all the tests performed in this work. The incubation time is enough to ascertain that the organism has reached its maximum concentration. The maximum halo to be obtained is measured at the same exposure period, but within varying degrees of concentrations of chemical, as stated in Table 4, and can be determined as the media of all measurements beyond MIC.

QSAR model construction and statistical analysis

Herein, it is important to state that we have carried out a minimum least squares procedure, employing a linear combination of chemical indexes, from three to six, in the form EC_{50}(calc.) = $\sum[C_i \times MI_i]$, where $i = 3$ to 6, C_i is a statistical adjustment coefficient, and MI_i is the chosen molecular descriptor or molecular index from the set of ten possible. From a full set of ten probable descriptors, giving a combination of 1200 (taking 3 of 10 possible) + 210 (taking 4 of 10 possible) + 252 (taking 5 of 10 possible) + 210 (taking 6 of 10 possible) = 1872 possibilities, and just three sets of chemical descriptors have accurate statistics. In this statistical search, if we chose a square matrix, this is an eight MI equation for eight possible chemical compounds (**4a–h**), we are defining an analytic resolution of the system. This latter implies that we are sure that these chosen variables are responsible of the behaviour of the system. Thus, the statistical approach is in charge to look forward into the sample space, in order to gather the important chemical descriptors and not the analytic solution of the system that should be doubtful by definition. In this assumption it has been decided not to test more descriptors than chemical compounds in order to avoid overestimation. All these were carried out to statistically identify the best set of chemical indexes and the results evidently show that only three equations have the level to be considered as confidant models. The latter was ascertained though the analysis of the correlation coefficient and also the adjusted

correlation coefficient, both being more than 0.98. Besides, the F coefficient is another confidence parameter for these means, since those three sets of descriptors were chosen to be with an F of more than 1000 units. Multiple linear regression (MLR) least squares analysis was employed to obtain the equations, which is implemented in the Analyse-it program provided in Excel software. Herein it is important to mention that just 1 of 1200 sets of three chemical indexes, 2 of 210 sets of four chemical indexes, 9 of 252 sets of five chemical indexes, and 15 of 210 sets of six chemical indexes, reached the desired statistical threshold of $R^2 > 0.99$ and R^2(adj) > 0.98, and just 3 sets of six chemical descriptors, of the overall sample, have passed through also the F > 1000 statistical threshold.

Acknowledgements

References

1 J. L. Shennan, *Biodeterior*, [Sel. Pap. Int. Biodeterior. Symp.], 7th, 1988, 248–255.
2 C. C. Gaylarde, F. M. Bento and J. Kelley, *Rev. Microbiol.*, 1999, **30**, 1–10.
3 H. A. Videla, *Manual of biocorrosion*, CRC Press, Boca Raton, 1996.
4 J. W. Costerton, *Biofouling Biocorros. Ind. Water Syst.*, 1994, 1–14.
5 S. Stolte, S. Abdulkarim, J. Arning, A. K. Blomeyer-Nienstedt, U. Bottin-Weber, M. Matzke, J. Ranke, B. Jastorff and J. Thoming, *Green Chem.*, 2008, **10**, 214–224.
6 S. Stolte, J. Arning, U. Bottin-Weber, M. Matzke, F. Stock, K. Thiele, M. Uerdingen, U. Welz-Biermann, B. Jastorff and J. Ranke, *Green Chem.*, 2006, **8**, 621–629.
7 S. Stolte, J. Arning, U. Bottin-Weber, A. Muller, W. R. Pitner, U. Welz-Biermann, B. Jastorff and J. Ranke, *Green Chem.*, 2007, **9**, 760–767.
8 A. Garcia-Lorenzo, E. Tojo, J. Tojo, M. Teijeira, F. J. Rodriguez-Berrocal, M. P. Gonzalez and V. S. Martinez-Zorzano, *Green Chem.*, 2008, **10**, 508–516.
9 A. Arce, M. J. Earle, H. Rodriguez, K. R. Seddon and A. Soto, *Green Chem.*, 2009, **11**, 365–372.
10 J. D. Holbrey, I. Lopez-Martin, G. Rothenberg, K. R. Seddon, G. Silvero and X. Zheng, *Green Chem.*, 2008, **10**, 87–92.
11 D. J. Couling, R. J. Bernot, K. M. Docherty, J. K. Dixon and E. J. Maginn, *Green Chem.*, 2006, **8**, 82–90.
12 K. M. Docherty and C. F. Kulpa, *Green Chem.*, 2005, **7**, 185–189.
13 J. R. Harjani, R. D. Singer, M. T. Garciac and P. J. Scammells, *Green Chem.*, 2009, **11**, 83–90.
14 J. R. Harjani, J. Farrell, M. T. Garcia, R. D. Singer and P. J. Scammells, *Green Chem.*, 2009, **11**, 821–829.
15 B. Jastorff, K. Molter, P. Behrend, U. Bottin-Weber, J. Filser, A. Heimers, B. Ondruschka, J. Ranke, M. Schaefer, H. Schroder, A. Stark, P. Stepnowski, F. Stock, R. Stormann, S. Stolte, U. Welz-Biermann, S. Ziegert and J. Thoming, *Green Chem.*, 2005, **7**, 362–372.
16 K. J. Kulacki and G. A. Lamberti, *Green Chem.*, 2008, **10**, 104–110.
17 K. Kummerer, *Green Chem.*, 2007, **9**, 899–907.
18 S. Morrissey, B. Pegot, D. Coleman, M. T. Garcia, D. Ferguson, B. Quilty and N. Gathergood, *Green Chem.*, 2009, **11**, 475–483.
19 S. Stolte, M. Matzke, J. Arning, A. Boschen, W. R. Pitner, U. Welz-Biermann, B. Jastorff and J. Ranke, *Green Chem.*, 2007, **9**, 1170–1179.
20 B. Jastorff, R. Stormann, J. Ranke, K. Molter, F. Stock, B. Oberheitmann, W. Hoffmann, J. Hoffmann, M. Nuchter, B. Ondruschka and J. Filser, *Green Chem.*, 2003, **5**, 136–142.
21 O. Lopez, J. G. Fernandez-Bolanos and M. V. Gil, *Green Chem.*, 2005, **7**, 431–442.
22 E. N. Petersen, *Acta Psychiatr. Scand.*, 1992, **86**, 7–13.

23 M. Matzke, S. Stolte, K. Thiele, T. Juffernholz, J. Arning, J. Ranke, U. Welz-Biermann and B. Jastorff, *Green Chem.*, 2007, **9**, 1198–1207.

24 A. A. Bulich, K. K. Tung and G. Scheibner, *J. Biolumin. Chemilumin.*, 1990, **5**, 71–77.

25 C. Hansch, D. Hoekman, A. Leo, D. Weininger and C. D. Selassie, *Chem. Rev.*, 2002, **102**, 783–812.

26 J. Arning, S. Stolte, A. Boschen, F. Stock, W. R. Pitner, U. Welz-Biermann, B. Jastorff and J. Ranke, *Green Chem.*, 2008, **10**, 47–58.

27 S. O. Podunavac-Kuzmanovic, D. D. Cvetkovic and D. J. Barna, *Int. J. Mol. Sci.*, 2009, **10**, 1670–1682.

28 E. L. Willighagen, H. Denissen, R. Wehrens and L. M. C. Buydens, *J. Chem. Inf. Model.*, 2006, **46**, 487–494.

29 F. Godinez-Salomon, J. M. Hallen-Lopez, H. Hopfl, A. Morales-Pacheco, H. I. Beltran and L. S. Zamudio-Rivera, *Green Chem.*, 2005, **7**, 716–720.

30 F. Briens, R. Bureau, S. Rault and M. Robba, *SAR QSAR Environ. Res.*, 1994, **2**, 147–157.

31 G. F. Whale and T. S. Whitham, *Soc. Pet. Eng. J.*, 1991, **23357**, 355–363.

32 B. Johnson, in *Small-scale Freshwater Toxicity Investigations*, 2005, pp. 69–105.

33 K. L. E. Kaiser and V. S. Palabrica, *Water Pollut. Res. J. Can.*, 1991, **26**, 361–431.

34 *Alternatives to Animal Use in Research Testing and Education, U. S. Congress, Office Of Technology Assessment.*, U.S. Government Printing Office, Washington, DC, 1986, OTA-BA-273.

35 *Microtox Tabulations of Pure Chemical Compounds*, Strategic Diagnostics Inc., Newark, DE, 2003.

36 R. McWeeny, *Phys. Rev.*, 1962, **126**, 1028–1034.

37 R. Ditchfie, *Mol. Phys.*, 1974, **27**, 789–807.

38 J. L. Dodds, R. McWeeny and A. J. Sadlej, *Mol. Phys.*, 1977, **34**, 1779–1791.

39 K. Wolinski, J. F. Hinton and P. Pulay, *J. Am. Chem. Soc.*, 1990, **112**, 8251–8260.

40 A. K. Jameson and C. J. Jameson, *Chem. Phys. Lett.*, 1987, **134**, 461–466.

41 W. Mabey and T. Mill, *J. Phys. Chem. Ref. Data*, 1978, **7**, 383–415.

42 C. Hansch, J. E. Quinlan and Lawrence.Gl, *J. Org. Chem.*, 1968, **33**, 347–350.

43 H. J. M. Verhaar, E. U. Ramos and J. L. M. Hermens, *J. Chemom.*, 1996, **10**, 149–162.

44 K. Legierse, H. J. M. Verhaar, W. H. J. Vaes, J. H. M. De Bruijn and J. L. M. Hermens, *Environ. Sci. Technol.*, 1999, **33**, 917–925.

45 R. D. van Anholt, T. Spanings, W. Koven and S. E. W. Bonga, *Am. J. Physiol. Regul. Integr. Comp. Physiol.*, 2003, **285**, R1098–1106.

46 Garc, J. a-Heredia, M. s. Herv, M. la Rosa and J. Navarro, *Planta*, 2008, **228**, 89–97.

47 N. Nasybullina, *Pharm. Chem. J.*, 1999, **33**, 88–93.

48 M. B. K. Bandara, H. Zhu, P. R. Sankaridurg and M. D. P. Willcox, *Invest. Ophthalmol. Visual Sci.*, 2006, **47**, 4453–4460.

49 H. T. D. Leinen, DE), Rudolf Lehmann, (Leichlingen, DE), Hans-juergen Klueppel, (Duesseldorf, DE), 1989. *Salicylic acid amides, their use, and a process for their production*. United States, 4795832.

50 M. Herrmann, *J. Clin. Invest.*, 2003, **112**, 149–151.

51 L. E. Rosenberg, A. L. Carbone, U. R∧mling, K. E. Uhrich and M. L. Chikindas, *Lett. Appl. Microbiol.*, 2008, **46**, 593–599.

52 T. Gebel, E. Lechtenberg-Auffarth and C. Guhe, *Reprod. Toxicol.*, 2009, **28**, 188–195.

53 Bruker, *SMART: Bruker Molecular Analysis Research Tool*, 2000, Version 5.618.

54 Bruker, *SAINT+NT*, 2001, Version 6.04.

55 Bruker, *SHELX-TL NT*, 2000, Version 6.10.

56 G. M. Sheldrick, *SHELX-97, Program for Crystal Structure Solution*, 1997, SHELX-97.

57 L. Farrugia, *J. Appl. Crystallogr.*, 1999, **32**, 837–838.

58 M. Nardelli, *J. Appl. Crystallogr.*, 1995, **28**, 659–659.

59 L. Farrugia, *J. Appl. Crystallogr.*, 1997, **30**, 565–565.

60 M. J. Frisch, G. W. Trucks, H. B. Schlegel, G. E. Scuseria, M. A. Robb, J. R. Cheeseman, V. G. Zakrzewski, J. A. Montgomery, Jr., R. E. Stratmann, J. C. Burant, S. Dapprich, J. M. Millam, A. D. Daniels, K. N. Kudin, M. C. Strain, O. Farkas, J. Tomasi, V. Barone, M. Cossi, R. Cammi, B. Mennucci, C. Pomelli, C. Adamo, S. Clifford, J. Ochterski, G. A. Petersson, P. Y. Ayala, Q. Cui, K. Morokuma, D. K. Malick, A. D. Rabuck, K. Raghavachari, J. B. Foresman, J. Cioslowski, J. V. Ortiz, A. G. Baboul, B. B. Stefanov, G. Liu, A. Liashenko, P. Piskorz, I. Komaromi, R. Gomperts, R. L. Martin, D. J. Fox, T. Keith, M. A. Al-Laham, C. Y. Peng, A. Nanayakkara, C. Gonzalez, M. Challacombe, P. M. W. Gill, B. G. Johnson, W. Chen, M. W. Wong, J. L. Andres, M. Head-Gordon, E. S. Replogle and J. A. Pople, *GAUSSIAN 98 (Revision A.7)*, Gaussian, Inc., Pittsburgh, PA, 1998.

61 A. D. Becke, *Phys. Rev. A: At., Mol., Opt. Phys.*, 1988, **38**, 3098–3100.

62 A. D. Becke, *J. Chem. Phys.*, 1993, **98**, 5648–5652.

63 C. T. Lee, W. T. Yang and R. G. Parr, *Phys. Rev. B: Condens. Matter*, 1988, **37**, 785–789.

64 J. P. Perdew, *Phys. Rev. B: Condens. Matter*, 1986, **33**, 8822–8824.

65 P. d'Antuono, E. Botek, B. Champagne, M. Spassova and P. Denkova, *J. Chem. Phys.*, 2006, **125**, 144309.

66 D. Vikic-Topic and L. Pejov, *J. Chem. Inf. Comput. Sci.*, 2001, **41**, 1478–1487.

67 J. P. Foster and F. Weinhold, *J. Am. Chem. Soc.*, 1980, **102**, 7211–7218.

68 A. E. Reed and F. Weinhold, *J. Chem. Phys.*, 1983, **78**, 4066–4073.

69 A. E. Reed, R. B. Weinstock and F. Weinhold, *J. Chem. Phys.*, 1985, **83**, 735–746.

This journal is © The Royal Society of Chemistry 2010